

MEASUREMENT OF KEY PARAMETERS FOR EAST NEUTRAL BEAM INJECTOR *

Yongjian Xu, Chundong Hu, Sheng Liu, Zhimin Liu, Yahong Xie, Peng Sheng, Lizhen Liang
 Institute of Plasma Physics, Chinese Academy of Sciences, Hefei, China, 230031

Abstract

Neutral beam injection is recognized as one of the most effective means of plasma heating. The target values of EAST neutral beam injector (NBI) are beam energy 50-80keV, injection beam total power 2-4 MW, beam pulse width 10-100s. The beam power will deposit on the beam collimator due to the beam divergence and it will cause heat damage to heat load components, or even destroy the entire NBI system. In order to decrease the risk, the key parameters of NBI, such as divergence angle, beam power density distribution, neutralizing efficiency, the beam power deposited on the heat load components, should be assessed. In this article, the calculation principle and experimental results are given. This results direct the operation parameter optimization of EAST NBI and lay a solid foundation for realization of plasma heating for EAST.

INTRODUCTION

Achievement of the ignition of fusion plasmas is one of the important subjects of plasma heating. It is well known widely that Neutral beam injection (NBI) is the most effective method for effective plasma heating and has been also verified to be applicable for current drive. As the first full superconducting non-circular cross section Tokomak in the world, EAST is used to explore the forefront physics and engineering issues on the construction of Tokomak fusion reactor [1-3]. According to the research plan of the EAST physics experiment, two sets of neutral beam injector will be built and operational in 2014. The target values of EAST NBI are beam energy 50-80keV, injection beam total power 2-4 MW, beam pulse width 10-100s [4-9]. The beam power will deposit on the beam collimator due to the beam divergence and it will cause heat damage to heat load components, or even destroy the entire NBI system. In order to decrease the risk, the key parameters of NBI, such as divergence angle, beam power density distribution, beam power deposition distribution and neutralizing efficiency, should be assessed. In this paper, the calculation principles and the experimental results of divergence angle, beam power density distribution, neutralization efficiency are given respectively. It is helpful to direct the operation parameter optimization of EAST NBI.

PRINCIPLES AND METHODS

Calculation of Beam Divergence Angle

Main components of the NBI system are two high-

*Work supported by the National Magnetic Confinement Fusion Science Program of China (2013GB101000) and the Presidential Foundation of the Hefei Institutes of Physical Science Chinese Academy of Sciences (Grant No. YZJJ201309).

current ion sources, control system, beam diagnosis system, vacuum system, gas supply system, cooling water system and so on. The ion source, which is the key device of EAST-NBI, consists of an arc chamber and a beam accelerator. The accelerator of EAST-NBI consists of four-grid electrostatic exaction accelerated systems, which are plasma grid (PG), gradient grid (GG), suppressor grid (SG) and exit grid (EG). Every electrode is composed of four sub-electrodes (i+,i-,i+2,i-2) and the assembling schematic diagram of every electrode is given by Fig.1. Figure1 shows that all sub-electrodes (i+, i+2, i-, i-2) focus to one point along the beam line. The distribution of beam intensity emitted by arbitrary point source of the electrode in space is

$$I = I_0 \exp\left(-\frac{2r^2}{w^2}\right) \quad (1)$$

Not considering the plasma nonuniformity in arc chamber, the beam intensity extracted by all the grids in x and y direction is the same. Establish a coordinate system as shown in Fig.2.

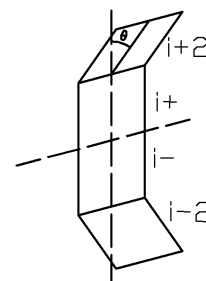


Figure 1: The assembling schematic diagram of every electrode (θ is the incident angle of beam emitted from the centre position of sub-electrode (i+2, i-2)).

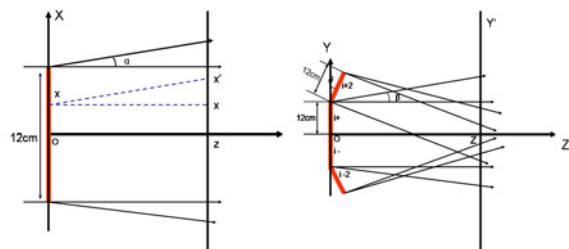


Figure 2: Geometric relationship of electrodes in X and Y direction (α and β is the divergence angle in X and Y direction, respectively).

The beam intensity of x emitted from x direction electrode is

$$I_{x^*} = \int_{-6}^6 I_0 \exp\left[-\frac{2(x^*-x)^2}{(z^* \tan \alpha)^2}\right] dx \quad (2)$$

The beam intensity of y point emitted by total electrode can be written

$$I_y = \int_{-12}^{24} I_0 \exp\left[-\frac{2(y'-y+z*\tan\theta)^2}{(z*\tan\beta)^2}\right] dy + \int_0^{12} I_0 \exp\left[-\frac{2(y'-y)^2}{(z*\tan\beta)^2}\right] dy + \int_{-12}^0 I_0 \exp\left[-\frac{2(y'-y)^2}{(z*\tan\beta)^2}\right] dy + \int_{-24}^{-12} I_0 \exp\left[-\frac{2(y'-y-z*\tan\theta)^2}{(z*\tan\beta)^2}\right] dy \quad (3)$$

Using the equation above, the beam intensity of all the points in z diagnosis plane can be obtained. Take $\theta = 1^\circ 5'$, $\alpha = 0.6^\circ$, $\beta = 1.2^\circ$, the beam intensity distribution can be obtained in different key components along beam transmission direction.

The thermocouples are installed in the calorimeter according to certain layout. The temperature rise can be recorded during the beam hits the calorimeter. The thermocouples in individual row/column of x/y direction have been chosen for beam divergence angle measurement. Fig.3 gives the temperature rise distribution and fitting curve. After normalization of the data shown in Figure 3, comparing the normalized temperature rise distribution fitting curve with the beam intensity distribution curve, the divergence angle of the most similar beam intensity distribution curve is the beam divergence angle.

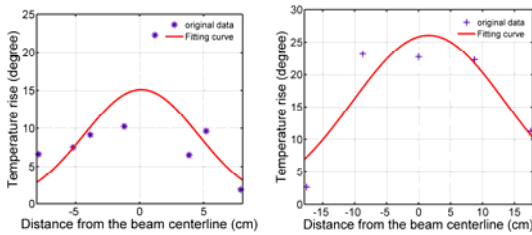


Figure 3: the temperature rise distribution and fitting curve in individual row/column of x/y direction (Left: X direction, Right: Y direction).

Calculation of Beam Power Density Distribution

Take any point of the plate as the study object. When the beam hit the plate, its energy of beam mainly transform into thermal energy and transmit along the plate. The power density of plate surface is p, assumed conversion efficiency of 100%, and then the magnitude of heat flux vector q is equal to p. The temperature of plate will vary with spatial and time, so the temperature field is a function of spatial and time

$$\theta = \frac{2q_w \sqrt{\alpha\tau} / \pi}{\lambda} \exp\left(\frac{-z^2}{4\alpha\tau}\right) - \frac{q_w z}{\lambda} \left(1 - \operatorname{erf}\left(\frac{z}{2\sqrt{\alpha\tau}}\right)\right) \quad (4)$$

Here q_w is heat flux boundary condition, τ is time, α is thermal diffusivity, λ is the thermal conductivity of calorimeter, z is the distance from the surface of calorimeter to the thermocouple. So the power density can be obtained when the temperature rise has been measured at some time τ .

$$q_w = \frac{\lambda\theta}{2\sqrt{\alpha\tau} / \pi \exp\left(\frac{-z^2}{4\alpha\tau}\right) - z\left(1 - \operatorname{erf}\left(\frac{z}{2\sqrt{\alpha\tau}}\right)\right)} \quad (5)$$

According to the boundary conditions, the power deposited on the calorimeter can be obtained using surface integral.

$$P = \iint_s q_w dx dy \quad (6)$$

Calculation of Beam Power Deposition Distribution

According to the cooling water flow rate and the temperature rise obtained by flow meter and differential temperature transducer, the power deposition of each heat-loading component can be calculated. The typical cooling water temperature rise was given by Fig.4. We can find that the temperature rise is a function of time, so the power deposited on the heat-loading component can be written

$$P = c_p m' \int_0^\infty T(t) dt \quad (7)$$

here, c_p is the specific heat of water, m' is the cooling water mass flow of heat-loading component, $T(t)$ is temperature rise of cooling water.

Considering the acquisition time t_f in each shot, the Equation 7 can be written

$$P = c_p \int_0^{t_f} m' T(t) dt + c_p \int_{t_f}^\infty m' T(t) dt \quad (8)$$

Due to the limit of acquisition time, acquisition time t_f is less than 10 minutes in general. The cooling water temperature can not return to the initial temperature (see Figure7). The curve of temperature drop with an exponential decay can be observed in the Fig.7, so the Equation 8 can be written

$$P = c_p \int_0^{t_f} m' T(t) dt + c_p \int_{t_f}^\infty m' a \exp(-bt) dt \quad (9)$$

here, a, b is the coefficient of exponential function and a, b can be obtained by data fitting. Measure real-time cooling water temperature rise and flow rate, the power deposition on the each heat-loading component can be obtained using Eq.9.

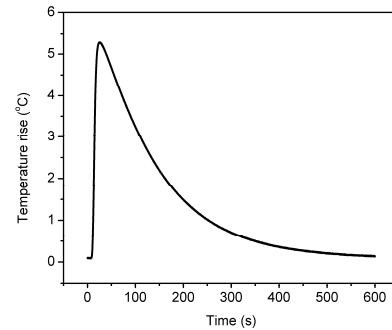


Figure 4: the typical cooling water temperature rise of heat-loading component.

Calculation of Neutralization Efficiency

Neutralization efficiency can be obtained by measuring the power deposited on the calorimeter

$$\eta = \frac{P_{on}}{P_{off}} \quad (10)$$

Where η is neutralization efficiency, P_{on} and P_{off} are the power deposited on the calorimeter when the bending magnet is on and off, respectively. P_{on} and P_{off} can be got using Eq.10.

RESULTS AND DISCUSSIONS

According to the data obtained from the thermocouple installed in the calorimeter, the power density distribution and divergence angle can be obtained (see Fig.5). Fig.5 shows that the beam has a relative good profile and beam divergence angle. According to the power density distribution given by Fig.5 and the boundary conditions of calorimeters ($x \in [-12, 12], y \in [-24, 24]$), the beam power deposited on calorimeter q_c can be obtained using Eq.6.

$$q_c = 1.69MW$$

q_c is about 85 percent of $V_{acc} * I_{acc}$ and it is consistent with the results measured by water flow calorimetry system[10]. Figure 6 gives the relationship between divergence angle and perveance. Figure 6 shows that (1) EAST-NBI ion source has a wide operation window, (2) the optimal perveance is about 2.8 μ -perv, (3) the highest perveance is 3.1 μ -perv and it has reached the design parameter of ion source for 10×48 cm beam extraction area.

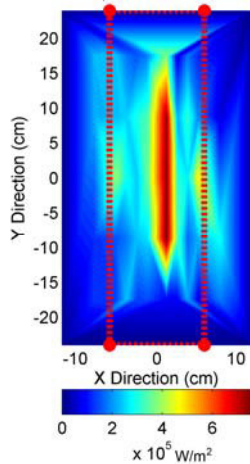


Figure 5: the beam intensity distribution of calorimeter (the area of red dotted bordered rectangle is equal to the extraction area of ion source) ($V_{acc}=66kV, I_{acc}= 30A,$ pulse length=0.37s, $\alpha=0.62^\circ, \beta=1.66^\circ$)

Beam carrying energy deposits on each heat-load components and energy deposition ration has been shown in Fig.7. It shows that: (1) energy deposition ration can indicate whether the ion source works on the optimal operation window; (2) energy deposition ration is an evidence for long pulse and high power beam extraction; (3) in terms of the power deposited on the calorimeter in the state of magnet on and off, the neutralizing efficiency can be obtained, neutralizing efficiency is key parameter for calculation of the energy injected into the plasma.

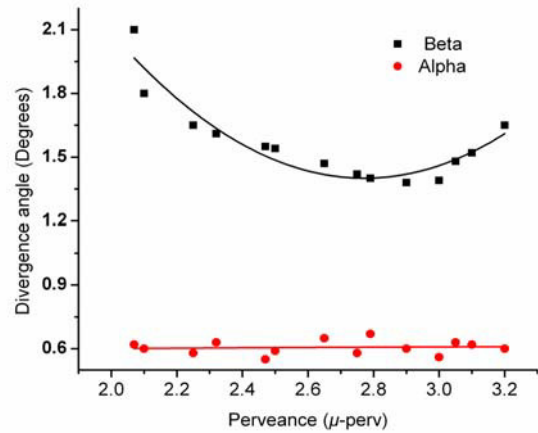


Figure 6: Divergence angle as a function of perveance (50kV, H-Beam, beam extraction area: $10 \times 48cm, \theta=1.5^\circ$)

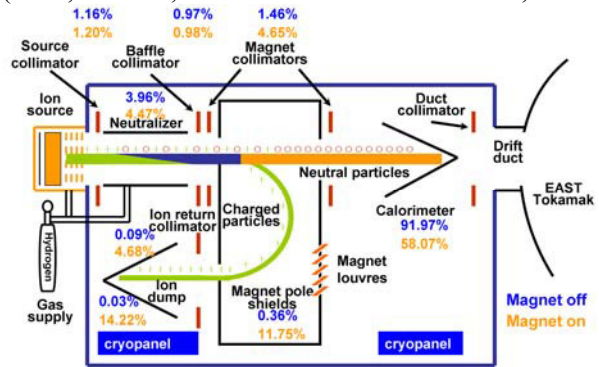


Figure 7: beam power deposition distribution on heat-loading components (50keV, 31.5A, H-Beam, beam extraction area: $10 \times 48cm, \theta=1.5^\circ$)

CONCLUSION

The experimental results of key parameters shown above can direct the operation parameter optimization of EAST NBI, in the meantime the obtaining of key parameters indicates that EAST NBI has an ability of heating plasma.

REFERENCES

- [1] Y.X. Wan, Nucl. Fusion, 40, 1057(2000).
- [2] J.G. Li, B.N. Wan, Nucl. Fusion, 51, 094007(2011).
- [3] B.N. Wan, Nucl. Fusion, 49, 104011(2011).
- [4] C.D. Hu, Plasma Sci. Technol., 14,567(2012).
- [5] Y. J. Xu, C. D. et al., Chin. Phys.Lett.29, 035201(2012).
- [6] C.D. Hu, Plasma Sci. Technol., 14,871(2012).
- [7] C.D. Hu, Y.H. Xie, Plasma Sci. Technol, 14, 75 (2012).
- [8] Y.J. Xu, C.D.Hu, et al., J. Fusion Energ. 32, 589 (2013).
- [9] Y.J. Xu, C.D. Hu, et al., J. Fusion Energ. 30, 94 (2011).
- [10] L. Yu, C.D. Hu, et al., Fusion Energ. 32, 547 (2013).